

Solvent-induced lone pair activity tuning and vapoluminescence in a Pt₂Pb cluster^{†&}

Jesús R. Berenguer,^a Elena Lalinde,^{*a} Antonio Martín,^b M. Teresa Moreno,^{*a} Santiago Ruiz,^a Sergio Sánchez^a and Hamid R. Shahsavari^a

We report a novel cluster, $[\{\text{Pt}(\text{C}_6\text{F}_5)(\text{bzq})\}_2\text{Pb}(\text{Spy})_2]$ **1**, that displays reversible vapoluminescence to specific organic vapours; this behaviour can be related to the stereochemical activity of the lone pair around the Pb^{II} in the ground state and to the distinct distortion of the coordination environment (**1** and **1**-solvent) upon photoexcitation.

Controlling the photoluminescence of transition-metal complexes by external stimuli is currently attracting widespread interest due to the possibility of obtaining photofunctional materials. In this context, the development of vapochromic or vapoluminescent materials, which show solid-state reversible colour changes in response to volatile organic compounds (VOCs), has received increased attention in recent years.^{1, 2} In this field, most of the reported materials are based on Pt^{II},¹⁻³ and Au^{II}.^{2, 4} compounds, though some interesting heterometallic systems [mainly Au-M (M = Tl,⁵ Ag,⁶ Cu^{7, 8})] have also appeared.

The spectral changes (absorption and emission) generally originate from a variety of mechanisms. For many systems they arise due to subtle modifications in the intermolecular interactions (metallophilic, $\pi\cdots\pi$ stacking, hydrogen bonding or C-H- π secondary contacts), associated with the sorption/desorption process. In other substances, particularly 3d metal complexes^{1, 9} and more rarely from Re^{II},¹⁰ and Pt^{II},¹¹ or Au^I complexes,⁸ the volatile molecule becomes coordinated/dissociated in the first coordination sphere of the metal ion, promoting a change in the geometry of a chromophore or rarely, generating isomerisation. Other less common materials only show a slight colour change in the ground state, but they change the luminescence drastically, mainly as result of exciplex formation between the host-framework and the solvent absorbed guest.¹² Though remarkable efforts have been devoted to understanding the origin of the vapochromic/vapoluminescent responses, on many occasions it is not a simple task. Therefore, further design of vapochromic materials with the aim of probing the relationship between solid state structures and the photophysical response still remains a considerable challenge.

We are interested in constructing luminescent materials based on different attractive interactions between Pt^{II} fragments and the borderline closed-shell Pb²⁺ ion.^{13, 14} We envisioned that the well known flexibility of Pb^{II} would impart fascinating luminescence properties through different degrees of activity of the lone pair $6s^2$.¹⁵ We recently found that $[\{\text{Pt}(\text{C}\equiv\text{CTol})_4\}\text{Pb}(\text{OH})_2]^{2-}$ showed reversible interaction with acetone with concomitant change in colour and emission. The lack of suitable crystals for an X-ray study and also the low stability of this complex prevented us to establish the nature of this behaviour.¹³ We report here the syntheses and remarkable structural and luminescence properties of a very stable Pt₂Pb cluster, which shows a dynamic and flexible core able to respond to solvent vapours through structural changes around the Pb^{II} ion.

When a suspension of $[\text{Pb}(\text{Spy})_2]$ in CH_2Cl_2 is treated with the solvate $[\text{Pt}(\text{bzq})(\text{C}_6\text{F}_5)(\text{acetone})]^{16}$ (1:2 molar ratio) it gradually dissolves, to afford a deep red solution from which a novel

luminescent (orange-red) compound, formulated as $[\{\text{Pt}(\text{C}_6\text{F}_5)(\text{bzq})\}_2\text{Pb}(\text{Spy})_2]$ (**1**), is isolated as an orange solid in high yield (Experimental in ESI). Interestingly, a visual and reversible change in the luminescence of the solid from orange-red to yellow-orange was observed in contact with a drop of acetone. We found the formation of two pseudopolymorphs depending on the solvent. Crystallization at low temperature from $\text{CH}_2\text{Cl}_2/n$ -hexane or acetone/ n -hexane produces orange crystals of stoichiometry $[\{\text{Pt}(\text{C}_6\text{F}_5)(\text{bzq})\}_2\text{Pb}(\text{Spy})_2]\cdot 1.5\text{CH}_2\text{Cl}_2$ (**1**·1.5 CH_2Cl_2) and $[\{\text{Pt}(\text{C}_6\text{F}_5)(\text{bzq})\}_2\text{Pb}(\text{Spy})_2(\text{acetone})]\cdot 1.5\text{acetone}$ (**2**·1.5acetone), respectively. The X-ray structure of **1**·1.5 CH_2Cl_2 (Fig. 1, Tables S1 and S2, ESI) revealed the formation of a bent $[\text{Pt}-\text{Pb}-\text{Pt } 140.753(9)^\circ]$ Pt₂Pb cluster with a very short Pt-Pb bond $[\text{Pt}(1)-\text{Pb } 2.7832(3) \text{ \AA}]$, supported by a bridging (μ - $\kappa\text{N},\text{S}$) pyridine-2-thiolate ligand (Spy⁻), and a longer Pt-Pb $[\text{Pt}(2)-\text{Pb } 3.1642(3) \text{ \AA}]$ bond, which is associated with the more unusual $6e^-$ (μ -1 $\kappa\text{N},\text{S};2\kappa\text{S}$) Spy⁻ bridging ligand. The short Pt-Pb distance is only slightly longer than the sum of the covalent radii (2.75 Å), and both distances are in the range reported for the relatively scarce number of species containing Pt-Pb bonds.^{13, 17} The Pb-N [2.565(5), 2.683(5) Å] and Pb-S(2) [2.797(1) Å] distances are comparable to those reported for $[\text{Pb}(\text{Spy}-\text{CF}_3)_2]$.¹⁸ The Pb-S(1) distance [3.545(2) Å] is far of bonding interaction. As has been previously noted,¹⁵ the exact geometry around Pb^{II} is not easy to define. In this system, the lead centre exhibits a primary “Pt₂N₂S” strongly distorted square pyramidal five-coordination, with the N atoms $[\text{N}(2)-\text{Pb}-\text{N}(4) 151.72(15)^\circ]$ and the Pt atoms $[\text{Pt}-\text{Pb}-\text{Pt } 140.753(9)^\circ]$ defining the basal positions and the bridging S(2) centre the apex (Fig. S1, ESI). The remarkable gap opposite to the sulphur centre is possibly occupied by the stereochemically active $6s^2$ lone pair (coordination as ψ -octahedron) (Fig. S2, ESI). Short *intra*- ($\text{Spy}\cdots\text{bzq}$) and *intermolecular* ($\text{bzq}\cdots\text{bzq}$) $\pi\cdots\pi$ contacts are also observed (Fig S3, ESI).

The structure of $[\{\text{Pt}(\text{C}_6\text{F}_5)(\text{bzq})\}_2\text{Pb}(\text{Spy})_2(\text{acetone})]\cdot 1.5\text{acetone}$ (**2**·1.5acetone) (Fig. 1, Tables S1 and S3, ESI) shows that one of the two and a half molecules of acetone present in the lattice is directly ligated to the Pb^{II} centre, causing a remarkable change in its coordination

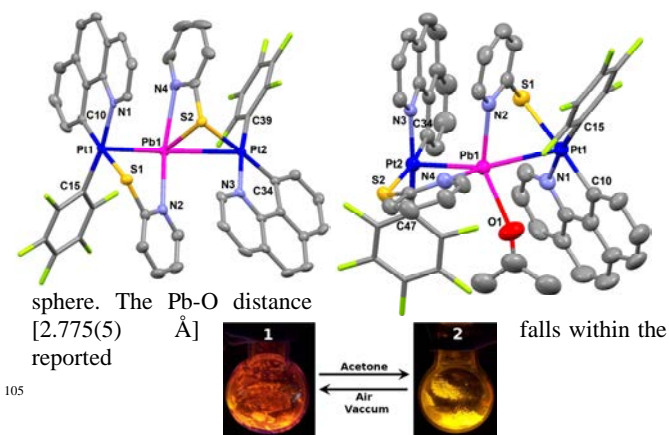


Fig 1. Molecular structures of **1**·1.5 CH_2Cl_2 (left) and of **2**·1.5 Me_2CO (right). Photographs showing the luminescence color change upon sorption of acetone vapour under UV light irradiation (365 nm).

range of Pb-O distances for the primary coordination sphere in lead(II) complexes.¹⁹ Further evidence for the coordination of

acetone is the presence of a $\nu(\text{C}=\text{O})$ band at 1696 cm^{-1} , lower than that of the free acetone ($\sim 1720\text{ cm}^{-1}$). Curiously, the coordination of the acetone causes the rupture of the $\text{Pb}^{\text{II}}\cdots\text{S}$ bond (Fig. S4, ESI) and enforces a small conformational change in the five membered ring (PbNCSPt), resulting in a final *cis* geometry of N atoms around Pb^{II} [$\text{N}(2)\text{-Pb-N}(4)$ $84.20(13)^\circ$] and also in a more acute Pt-Pb-Pt angle [$133.291(8)^\circ$] compared to that in **1**. This rearrangement seems to be accompanied by a decrease in the lone pair activity in relation to **1** (also supported by TD-DFT). Thus, in **2** the local $\text{Pt}_2\text{N}_2\text{O}$ environment around the Pb^{II} ion is more *holodirected*, and displays less asymmetric and slightly shorter (within average) Pb-N [$2.497(4)$, $2.568(4)\text{ \AA}$] and $\text{Pb}^{\text{II}}\text{-Pt}$ [$2.8401(3)$, $2.9790(3)\text{ \AA}$] distances in relation to those found in **1**. These changes seem to be responsible for the observed photoluminescent behaviour. In fact, despite the incorporation of a greater amount of acetone solvent (density: 2.046 2 vs $2.221\text{ g/cm}^3\text{ 1}$) both, the *intra* ($\text{Spy}^-\cdots\text{bzq}$) and *inter* ($\text{bzq}^-\cdots\text{bzq}$) $\pi\cdots\pi$ contacts are similar in both pseudopolymorphs (Fig. S3 and S5, ESI).

As noted above, there is no significant difference in the colour of **1** and **2**. Both complexes show similar patterns in the solid state UV-vis electronic spectra (Fig. S6, ESI), with the shoulder of the absorption maximum slightly red-shifted in **2** ($\sim 495\text{ 2}$ vs 480 nm 1). However, **1** (crystalline or powder) and the solvate **2** have different emission colours and efficiencies (Fig. S7 and Table 1 for details). The emission bands (620 1 , 580 nm 2) do not change significantly at low temperature and display similar excitation spectra, suggesting that the remarkable blue-shift in the emission of **2** in relation to **1** could be related to the occurrence of a smaller Stokes shift in **2**.

Interestingly, complex **1** can be converted to **2** through sorption of acetone vapour (Fig. 1). When powder **1** is exposed to Me_2CO vapour, the solid-state luminescence colour changes from orange-red (620 nm) to yellow-orange (580 nm) in a few minutes ($\sim 10\text{ min}$), indicating the transformation has occurred. On standing, the acetone was completely lost in $\sim 12\text{h}$, recovering **1**. The desolvation, when passing a stream of air onto the sample **2**, was monitored by emission spectroscopy (Fig. S8) and results showed a gradual change from **2**-x(acetone) to **1**, so we can not discard the formation of intermediate species. We note that the **2** to **1** process takes place also by grinding **2** in a ceramic mortar (Fig. S9, ESI). Subsequent treatment of the crushed powder **1** with a drop of acetone leads again to the initial yellow-orange emissive phase (**2**-x(acetone)). The characteristic emission of **1** and **2** can be recovered several times by sequential and repetitive paths (grinding and treatment with acetone). The loss of acetone molecules, determined by TGA (Fig S10, ESI), fits to a molar ratio acetone/**1** of *ca.* $2:1$ [**2**-x(acetone), $x \sim 1$]. Conclusively, powder X-ray diffraction (PXRD) diagrams were recorded for solid samples of **1** and **1** exposed to saturated acetone vapour (**2**-x(acetone)) at 298 K . The diffraction peaks correspond approximately to those calculated from the diffraction data of the single crystal X-ray analysis of $1\cdot 1.5\text{CH}_2\text{Cl}_2$ and $2\cdot 1.5\text{acetone}$, respectively (Fig. S11, ESI).

Vapour response of **1** to other donor solvents such as MeCN, MeOH and THF is also relatively fast [MeCN ($\sim 10\text{ min}$) > MeOH (20 min) > THF (30 min)], provoking a distinct shift to the yellow region in the photoemission (Fig. S12 and S13, Table 1). However, no-donor solvents such as toluene, hexane or even diethyl-ether do not trigger a response. The solvated products, **1**-x(solvent), possibly similar to **2**-x(acetone), were obtained as pure phases by addition of a drop of the respective solvent to **1**. The desolvation process for **1**-THF (Fig. S8b), examined by

emission spectroscopy, followed a similar pattern to **2**-x(acetone). It is assumed that these donor solvents L are able to approach to the Pb^{II} , causing a change in the local environment from a distorted *hemidirected* " $\text{Pt}_2\text{N}_2\text{S}$ " to a more symmetrical " $\text{Pt}_2\text{N}_2\text{L}$ ". As listed in Table 1, in the solvates the phosphorescence yields are smaller and the calculated non-radiative constants, k_{nr} , are larger than those of **1**. The presence of a more rigid $6e^-\text{Spy}^-$ bridging ligand in **1** could explain the lower observed k_{nr} value.

Table 1 Luminescence Properties of [$\{\text{Pt}(\text{C}_6\text{F}_5)(\text{bzq})\}_2\text{Pb}(\text{Spy})_2$]

	T ^a /K	$\lambda_{\text{em}}/\text{nm}$	ϕ	$\tau/\mu\text{s}$	$k_r^{[a]}$	$k_{\text{nr}}^{[b]}$
1	298	620	34	1.6	2.1×10^5	4.1×10^5
	77	616		5.2		
2	298	580	14	0.5	2.8×10^5	1.7×10^6
	77	577		9.3		
1 -MeCN	298	585	15	0.5	3.0×10^5	1.7×10^6
	77	570		11		
1 -MeOH	298	576	17	0.3	5.6×10^5	2.8×10^6
	77	575		12.9		
1 -THF	298	570	21	0.6	3.5×10^5	1.3×10^6
	77	563		7.7		

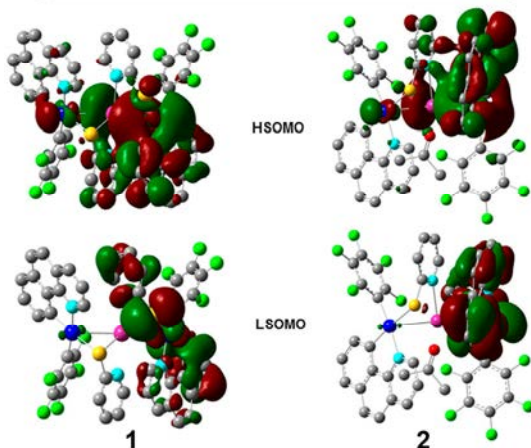
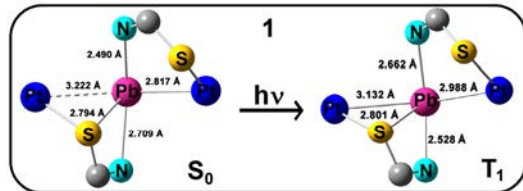
^[a] $k_r = \phi/\tau$. ^[b] $k_{\text{nr}} = 1/\tau(1-\phi)$

Complex **1** exhibits a similar UV-vis absorption profile in CH_2Cl_2 and in acetone solution (Fig. S14, ESI). The low energy absorptions at $400\text{-}500\text{ nm}$ are tentatively assigned to transitions having mixed configurations [$^1\text{IL}(\text{bzq})$ and ligand (Spy)-to-metal(Pt-Pb) charge transfer] on the basis of DFT calculations. In fluid solutions **1** is weakly emissive ($\lambda_{\text{max}}\text{ 620 nm}$) probably due to non-radiative decay favored by molecular motions (fluxionality averaging both Spy^- ligands in CH_2Cl_2 or simple coordination/decoordination of the solvent in acetone solution). After cooling to 77 K , the emission is enhanced and similar blue-shifts are observed in both solvents (570 nm , Fig. S15 and S16, ESI).

To gain insight into the properties of both pseudopolymorphs, DFT optimization of the ground (S_0) and the lowest excited state (T_1) were carried out for **1** and **2** (details are given in ESI, Tables S4-S9). The calculated structures reproduce reasonably well the X-ray structures, reflecting the very asymmetric Pb-Pt and Pb-N bonds found in **1** (Fig. S17, S18, ESI). Comparison of the bond lengths in the

Fig. 2 Optimized structures (S_0 and T_1 state) in **1** (top). MOs plots for the computed T_1 states of complexes **1** and **2** (bottom).

optimized S_0 state and the T_1 state for both complexes, reveals that upon photoexcitation complex **1** rearranges to a more symmetrical $\text{Pt}_2\text{N}_2\text{S}$ core (Fig. 2, top), whereas in the solvate complex **2**, the changes in the $\text{Pt}_2\text{N}_2\text{O}$ core are negligible. This result is in line with previous studies of s^2 complexes, which suggested that distortion in *hemidirected* structures is reduced (or even eliminated) in the excited state.²⁰ To investigate this, additional natural bond orbital (NBO) analysis (Table S8, ESI) were performed to estimate the hybridization of the lone pair on Pb^{II} ion, both in the S_0 and T_1 states. This study confirms, in the ground S_0 state, there is greater p-character in the asymmetrical complex **1** ($2.42\% \text{ p 1}$ vs $0.34\% \text{ p 2}$) and decreases in the corresponding T_1 state ($2.03\% \text{ p 1}$). Inspection of the HSOMO (Fig. 2, bottom), from which the emission is produced, indicates that in both complexes there is bonding character within the Pt-Pb-Pt entity and also a remarkable contribution from one of the π^* bzq ligands (Pt₂Pb $46\% \text{ bzq 41\% 1}$ vs Pt₂Pb $25\% \text{ bzq 66\% 2}$). The LSOMOs are primarily confined to one of the $\mu\text{-Spy}^-$ bridging ligands and



the associated Pt(bzq) fragment (μ -Spy 48% Ptbzq 50% **1** vs μ -Spy 35% Ptbzq 64% **2**). The calculated phosphorescence (560 nm **1**, 531 nm **2**) reproduces the observed trend and can be ascribed to an admixture of intraligand (bzq, more important in **2**) and ligand (Spy)-to-metal (Pt-Pb) charge transfer transitions. The different Stokes shift (4593 cm^{-1} **1** vs 3231 cm^{-1} **2**) reflects the smaller geometrical change in the excited state of the more symmetrical solvate **2** and is consistent with the observed blue shift in the emission.

In summary, complex **1** represents an unusual example of vapoluminescent lead-based material. X-ray and DFT studies suggest that the change in the emission colour of **1** upon uptake VOCs can be primarily attributed to a different distortion of the geometry around the lead center upon photoexcitation. Further studies of similar clusters are currently in progress to understand the role of the Pt fragments and the thiolates ligands in this mechanism assumption.

Acknowledgment. This work was supported by the Spanish MICINN (CTQ2008-06669-C02-01,02/BQU and a grant for S. R.). The authors also thank CESGA for computer support.

Notes and references

^aDepartamento de Química-Centro de Síntesis Química de La Rioja, (CISQ), Universidad de La Rioja, 26006, Logroño, Spain. E-mail: elena.lalinde@unirioja.es; teresa.moreno@unirioja.es. ^bDepartamento de Química Inorgánica, Instituto de Síntesis Química y Catálisis Homogénea, Universidad de Zaragoza-C.S.I.C., 50009 Zaragoza, Spain.

† Electronic Supplementary Information (ESI) available: Synthetic procedures, full set of characterization data, crystallographic, photophysical and theoretical data. CCDC 927150-927151. See DOI: 10.1039/b000000x/

& Dedicated to Professor Antonio Laguna on the occasion of his 65th birthday

- X. Zhang, B. Li, Z. H. Chen and Z. N. Chen, *J. Mater. Chem.*, 2012, **22**, 11427.
- Q. Zhao, F. Li and C. Huang, *Chem. Soc. Rev.*, 2010, **39**, 3007; O. S. Wenger, *Chem. Rev.*, 2013, 10.1021/cr300396p.
- K. M. C. Wong and V. W. W. Yam, *Coord. Chem. Rev.*, 2007, **251**, 2477; M. Kato, *Bull. Chem. Soc. Jpn.*, 2007, **80**, 287.
- X. He and V. W. W. Yam, *Coord. Chem. Rev.*, 2011, **255**, 2111.
- E. J. Fernández, A. Laguna, and J. M. López de Luzuriaga, *Coord. Chem. Rev.*, 2005, **249**, 1423.
- T. Lasanta, M. E. Olmos, A. Laguna, J. M. López-de-Luzuriaga and P. Naumov, *J. Am. Chem. Soc.*, 2011, **133**, 16358; E. J. Fernández, J.

- M. López-de-Luzuriaga, M. Monge, M. E. Olmos, R. C. Puelles, A. Laguna, A. A. Mohamed and J. P. Fackler Jr, *Inorg. Chem.*, 2008, **47**, 8069; A. Luquin, C. Bariáin, E. Vergara, E. Cerrada, J. Garrido, I. R. Matias and M. Laguna, *Appl. Organometal. Chem.*, 2005, **19**, 1232.
- J. Lefebvre, R. J. Batchelor and D. B. Leznoff, *J. Am. Chem. Soc.*, 2004, **126**, 16117.
- C. E. Strasser and V. J. Catalano, *J. Am. Chem. Soc.*, 2010, **132**, 10009.
- J. Lefebvre, J. L. Korcok, M. J. Katz and D. B. Leznoff, *Sensors*, 2012, **12**, 3669.
- H. Ikeda, T. Yoshimura, A. Ito, E. Sakuda, N. Kitamura, T. Takayama, T. Sekine and A. Shinohara, *Inorg. Chem.*, 2012, **51**, 12065.
- M. Albrecht, M. Lutz, A. L. Spek and G. van Koten, *Nature*, 2000, **406**, 970; A. Kobayashi, Y. Fukuzawa, H. C. Chang and M. Kato, *Inorg. Chem.*, 2012, **51**, 7508.
- Z. M. Hudson, C. Sun, K. J. Harris, B. E. G. Lucier, R. W. Schurko and S. Wang, *Inorg. Chem.*, 2011, **50**, 3447.
- J. R. Berenguer, A. Díez, J. Fernández, J. Forniés, A. García, B. Gil, E. Lalinde and M. T. Moreno, *Inorg. Chem.*, 2008, **47**, 7703.
- J. R. Berenguer, J. Fernández, E. Lalinde and S. Sánchez, *Chem. Commun.*, 2012, **48**, 384.
- L. Shimoni-Liuny, J. P. Glusker and C. W. Bock, *Inorg. Chem.*, 1998, **37**, 1853.
- J. R. Berenguer, E. Lalinde, M. T. Moreno, S. Sánchez and J. Torroba, *Inorg. Chem.*, 2012, **51**, 11665.
- J. M. Casas, J. Forniés, A. Martín, V. M. Orera, A. G. Orpen and A. Rueda, *Inorg. Chem.*, 1995, **34**, 6514; R. Usón, J. Forniés, L. R. Falvello, M. A. Usón and I. Usón, *Inorg. Chem.*, 1992, **31**, 3697; V. J. Catalano, B. L. Bennett and B. C. Noll, *Chem. Commun.*, 2000, 1413; A. L. Balch, E. Y. Fung, J. K. Nagle, M. M. Olmstead and S. P. Rowley, *Inorg. Chem.*, 1993, **32**, 3295; D. Heitmann, T. Pape, A. Hepp, Mück-Lichtenfeld, S. Grimme and F. Ekkehardt Hahn, *J. Am. Chem. Soc.*, 2011, **133**, 11118; H. Braunschweig, A. Damme, R. D. Dewhurst, F. Hupp, J. O. C. Jiménez-Halla and K. Radacki, *Chem. Commun.*, 2012, **48**, 10410.
- A. Sousa-Pedrares, M. I. Casanova, J. A. García-Vázquez, M. L. Durán, J. Romero, A. Sousa, J. Silver and P. J. Titler, *Eur. J. Inorg. Chem.*, 2003, 678.
- R. L. Davidovich, V. Stavila, D. V. Marinin, E. I. Voit and K. H. Whitmire, *Coord. Chem. Rev.*, 2009, **253**, 1316.
- A. Vogler and H. Nikol, *Pure Appl. Chem.*, 1992, **64**, 1311.